Journal of Catalysis 270 (2010) 146–152

Contents lists available at ScienceDirect

Journal of Catalysis

journal homepage: www.elsevier.com/locate/jcat

Design of supported cobalt catalysts with maximum activity for the Fischer–Tropsch synthesis

Johan P. den Breejen, Jelle R.A. Sietsma [1], Heiner Friedrich, Johannes H. Bitter, Krijn P. de Jong *

Inorganic Chemistry and Catalysis, Debye Institute for NanoMaterials Science, Utrecht University, NL-3584 CA Utrecht, The Netherlands

ARTICLE INFO

Article history:
Received 17 September 2009
Revised 14 December 2009
Accepted 15 December 2009
Available online 13 January 2010

Keywords:
Fischer–Tropsch synthesis
Cobalt catalysts
Particle size distribution
Cobalt on silica
NO calcination

ABSTRACT

The role of the cobalt particle size distribution in the Fischer–Tropsch (FT) reaction for supported Co catalysts was investigated. Using TEM histogram analyses and activity measurements of carbon nanofiber-supported catalysts, the TOF of discrete Co particle sizes was calculated. It was found that cobalt particles of 4.7 ± 0.2 nm are the most active in the FT reaction (1 bar, 220 °C), and a narrow Co particle size distribution is clearly essential to arrive at the maximum activity. We have approached this requirement for maximum FT activity with an 18 wt.% Co/SiO_2 catalyst prepared via impregnation, drying and calcination in NO/He. The more narrow Co particle size distribution (4.6 ± 0.8 nm) in Co/SiO_2 led to an activity enhancement of ~40% compared to Co/CNF (5.7 ± 1.4 nm), although some promoting effect of silica could not be excluded.

1. Introduction

In the Fischer–Tropsch (FT) reaction, synthesis gas (CO and H_2) is converted into higher hydrocarbons. Using this process, hydrocarbon fuels can be synthesized from variable sources (coal, gas and biomass), thus providing an alternative to fuels from crude oil. Active and selective catalysts for the FT reaction are mainly based on Co or Fe. Especially for Co, due to its higher price and lower availability, an effective use of the metal is required, which can be achieved by decreasing the metal particle size. However, for too small cobalt particle sizes a drop in activity is observed, as for example reported by Bartholomew [1,2] and Yermakov [3,4]. Hence, an optimal particle size is often reported. For example, Barbier et al. reached the highest weight-based activity with cobalt particle sizes of 5.5 nm [5]. Bezemer et al. showed an optimum cobalt particle size of 6 nm on carbon nanofibers (CNF) for FT experiments performed at 1 bar, $H_2/CO = 2$, 220 °C [6]. Our recent Steady-State Isotopic Transient Kinetic measurements (1.85 bar, $H_2/CO = 10$, 210 °C) with similar catalysts showed changes in coverages and residence times of FT intermediates, and among others the presence of irreversibly bonded CO for Co particle sizes smaller than 5–6 nm [7].

These catalysts were often prepared by impregnation, drying, calcination and reduction. This approach, in general, results in catalysts with a more or less broad distribution of the sizes of the cobalt crystallites. For a system with a size-independent surface-specific activity (Turn-Over Frequency, TOF), the surface-average particle size would be sufficient to describe a size–activity relationship. However, since for the Fischer–Tropsch reaction different particle sizes show different surface-specific activities [6,7], an analysis of the size–activity relationship on the basis of average Co particle sizes will be limited, and a refinement through the use of particle size distributions is required.

In the first part of this study, cobalt on carbon nanofiber catalysts are used as a model system. Carbon nanofibers were chosen because of their chemical inertness, which allows to study the intrinsic activity of cobalt particles. From cobalt size distribution curves and FT activities of eight catalysts, we estimate the intrinsic TOF for discrete particle sizes via an iterative analysis. The results are used to calculate the Co particle size at which maximum activity is reached.

In the second part, this knowledge is applied to synthesize a catalyst on a conventional oxidic support material (SiO_2) with a narrow Co particle size distribution close to the calculated optimal size. Approaches to synthesize a 'monodisperse' cobalt catalyst may involve impregnation, sometimes with the use of organic precursor complexes and/or chelating ligands [8–11] or the use of colloids [12,13]. Aqueous impregnation using a cobalt nitrate hexahydrate precursor is still most widely applied. The main reasons for the use of the nitrate precursor are cost-effectiveness, high loadings via single-step impregnation and easy removal of the ligand. However, the reduced catalysts prepared via this method show in general a low metal dispersion and broad particle size

* Corresponding author. Fax: +31 30 251 1027.
E-mail address: k.p.dejong@uu.nl (K.P. de Jong).
[1] Present address: Shell Global Solutions, NL-1030 BN Amsterdam, The Netherlands.

0021-9517/$ - see front matter © 2010 Elsevier Inc. All rights reserved.
doi:10.1016/j.jcat.2009.12.015

distribution. The poor dispersion of supported catalysts prepared via nitrate precursors has been ascribed to redistribution during drying or agglomeration during calcination. In a recent study, we showed that it is possible to prevent this redistribution by the use of a modified calcination treatment in NO/He flow [14–16]. Using this calcination procedure, we have been able to synthesize a highly loaded FT catalyst with a narrow particle size distribution from a nitrate precursor on a conventional silica support. The effect of the NO calcination on the cobalt oxide particle size distribution was studied and compared with the results found for an air-calcined catalyst. The reducibility of the small cobalt oxide crystallites prepared via NO calcination was investigated with XANES analysis. These catalysts were subsequently reduced and tested in the Fischer–Tropsch synthesis at 220 °C, 1 bar.

2. Materials and methods

2.1. Catalysts preparation

2.1.1. Co/CNF

The carbon nanofiber support (fishbone-type) with a fiber diameter of about 30 nm was obtained as described before [17]. The cobalt catalysts were synthesized using incipient wetness impregnation, in which cobalt loading (0.9–13 wt.%), cobalt precursor (cobalt nitrate or cobalt acetate) and solvent (water or ethanol) were varied. After impregnation, the catalysts were dried in air at 120 °C for 12 h. The cobalt on carbon nanofiber catalysts were reduced at 350 °C (5 °C min^{-1}) for 2 h in a flow of 33 vol.% hydrogen, which was followed by an oxidation treatment to CoO at room temperature by diffusion of air to the reactor, thereby preventing complete oxidation to Co_3O_4. This yielded Co/CNF catalysts with various average particle sizes (2.6–11 nm).

2.1.2. Co/SiO_2

The cobalt on silica catalysts were prepared via incipient wetness impregnation. Silica (Grace-Davison Davicat 1454SI silica gel, BET surface area = 500 m^2 g^{-1}, pore volume = 1.1 mL g^{-1} and 6 nm average pore size) was impregnated with an aqueous cobalt nitrate solution, to achieve a cobalt loading of 18 wt.%. Subsequently, the catalyst was dried by heating the samples from room temperature (RT) to 70 °C at a heating rate of 1 °C min^{-1} and kept at this temperature for 12 h. Next, the dried catalyst (100 mg) was calcined in a 100 mL min^{-1} flow of 1 vol.% NO in He. The sample was heated from RT to 240 °C at a rate of 1 °C min^{-1} and kept at this temperature for 1 h. For comparison, another batch of the catalyst was calcined in air following the same procedure of flow and ramp. The NO and air calcinations are abbreviated NC and AC, respectively.

A platinum promoted cobalt on silica catalyst was prepared via co-impregnation of an aqueous solution of platinum tetrammonium nitrate (0.05 wt.% Pt) (Aldrich) and cobalt nitrate hexahydrate (18 wt.% Co) (Merck). After impregnation, the catalyst was dried and calcined in NO/He or air as described earlier.

All catalysts (25 mg) were reduced at 550 °C (Co/SiO_2) or 450 °C (CoPt/SiO_2) with a heating rate of 5 °C min^{-1}, 2 h, in a 60 mL min^{-1} flow of 33 vol.% H_2 in N_2. Next, the catalysts were oxidized in air to CoO at room temperature.

2.2. Catalyst characterization

The reduced and oxidized catalysts were applied to a carbon support film via suspension in ethanol. The TEM measurements (bright-field mode) were conducted with a Tecnai 20 FEG microscope operating at 200 kV. The cobalt particle diameters from more than 200 particles for each sample were measured using iTEM software (Soft Imaging System GmbH). For non-symmetrical particle shapes, both the largest and shortest distance were measured to obtain an average value for the particle diameter. Since the cobalt particles show the CoO phase after the oxidation treatment mainly, as confirmed by XRD and XAS measurements, the cobalt metal particle sizes were calculated according to Eq. (1)

$$d(\mathrm{Co}) = \left(\frac{\rho(\mathrm{CoO})\cdot M_w(\mathrm{Co})}{\rho(\mathrm{Co})\cdot M_w(\mathrm{CoO})}\right)^{1/3}\cdot d(\mathrm{CoO}) \quad (1)$$

As the Co particle sizes in this study were small (<20 nm), it was assumed based on literature [18] that all catalysts showed FCC stacking only.

From the particle sizes, the diameter-weighted ($d_{DW} = (\sum n_i d_i)/\sum n_i$), surface-weighted ($d_{SW} = ((\sum n_i d_i^2)/\sum n_i)^{1/2}$) and volume-weighted ($d_{VW} = ((\sum n_i(\sum n_i d_i^3)/\sum n_i)^{1/3}$) average Co particle sizes were calculated [19]. The standard deviation ($\sigma = ((\sum(d_i - d_{SW})^2)/\sum n_i)^{1/2}$) was calculated assuming a Gaussian spread. Subsequently, the Co particle sizes were distributed over equally sized bins in the histogram analysis. A bin size of 0.50 nm was chosen, with a bin center ranging from 1.0, 1.5, 2.0, 2.5, . . . , 20 nm. To check the effect of binning, three other bins were used with different bin size (0.25 or 1.00 nm) and/or bin center. Since these analyses yielded virtually identical results, we only show the results obtained with the 0.5 nm bins. The histograms were normalized assuming spherical particles and subsequently fitted using a lognormal distribution [20].

XPS measurements on the Co/CNF samples were conducted with a Vacuum Generators XPS system (Al–K_α radiation). From the Shirley background normalized C(1s) and Co(2p) peaks, the cobalt oxide particle size was calculated [6,21,22]. Subsequently, the surface-average cobalt particle size was calculated by correcting for the contraction of CoO to Co as described earlier.

X-ray absorption spectroscopy (XAS) on the Co K-edge was performed at the DESY synchrotron (Hamburg, Germany) at beamline C (4.44 GeV, mean current 120 mA), using a Si(1 1 1) double crystal monochromator. As reference, a cobalt foil was measured simultaneously in a third ionization chamber. The calcined catalysts (50 mg) were diluted with 50 mg BN, pressed into a pellet and mounted in a dedicated transmission cell. The samples were *in situ* reduced in a ~200 mL min^{-1} hydrogen flow (33 vol.% H_2 in He) at either 450 °C or 530 °C for 2 h, with a ramp of 5 °C min^{-1}. The samples were subsequently cooled in an H_2 flow to liquid nitrogen (LN) temperature, at which temperature the spectra were measured. Next, the samples were heated to 220 °C, and CO was added to the flow of hydrogen (H_2/CO = 2 v/v). The FT reaction was performed for 2 h prior to a XAS measurement at LN temperature. Spectra of Co_3O_4, CoO and cobalt foil were measured as references. The absorption spectra were analyzed as described elsewhere [23,24]. The X-ray Absorption Near-Edge (XANES) part of the XAS measurements was used to determine the degree of reduction. To this end, principal component analysis by linear combination of the CoO and Co foil spectra was used to fit the whiteline intensity of the AC and NC catalysts.

2.3. Catalytic testing

The Fischer–Tropsch reaction was performed at 220 °C at 1 bar in a plug-flow reactor with an H_2/CO ratio of 2 v/v. Typically, 20 mg catalyst (90–150 μm), mixed with 200 mg SiC (200 μm), was loaded in the reactor in order to achieve isothermal plug-flow conditions. The calcined catalysts were *in situ* reduced at temperatures ranging from 350 to 600 °C, for 2 h, with a ramp of 5 °C min^{-1} in 20 mL min^{-1} H_2 and 40 mL min^{-1} Ar. Online gas chromatography analysis (C_1–C_{16}) was performed during the FT reaction to determine the activity and selectivity (wt.%) toward C_1 (methane) and

C_{5+} hydrocarbons. The activity was expressed as Cobalt-Time Yield (CTY, 10^{-5} mol_{CO} g_{Co}^{-1} s^{-1}). The reported activity and selectivity data are obtained after at least 20 h of FT synthesis and at 2% CO conversion.

3. Results and discussion

3.1. TEM histogram analysis and calculation of intrinsic TOF

The TEM images of eight Co/CNF catalysts with different cobalt particle sizes are provided in the Supplementary Information (SI) – A, together with their cobalt particle size histograms. An example of a TEM image, particle size distribution and its lognormal fit are provided in Fig. 1.

Details of the preparation, cobalt sizes and FT activities of these Co/CNF catalysts are shown in Table 1. Part of these results was taken from Bezemer et al. [6]. For the TEM particle sizes, both the diameter-weighted, surface-weighted and volume-weighted diameters were calculated.

The histograms were fitted using a lognormal fit to obtain the particle size distribution in the limit of an infinite number of size measurements. Based on these lognormal distributions and the overall activity of the eight catalysts, an estimate of the intrinsic surface-specific activity ($TOF_{i,n}$) for each particle size was made, using following procedure. First, the number of cobalt surface atoms per gram of cobalt in each bin for each catalyst was calculated. Next, an intrinsic surface-specific activity ($TOF_{i,n}$) was attributed to a specific Co particle size, *i.e.* the center of a histogram bin. As an initial guess for this intrinsic activity, the TOF-size relationship found by Bezemer et al. [6] was taken. Subsequently, this $TOF_{i,n}$ was multiplied by the number of cobalt surface atoms per gram cobalt present in the corresponding bin. Summation over all bins yielded a calculated activity (CTY) value. This procedure was performed for all catalysts, which enabled to compare a number of measured and calculated CTY values. In the last step, the intrinsic activity was iteratively changed to match measured and calculated CTY values. From the eventual estimated intrinsic activities, the Co particle size corresponding to the maximum activity was calculated. A detailed description of the analysis and calculations is provided in SI – B.

In Fig. 2A, an example of the estimated intrinsic TOF, for which the best fitting result was obtained, is shown as function of the Co particle size. Based on this, the weight-based activities (CTY) for various Co/CNF catalysts could be calculated. In Fig. 2B, this calculated CTY is plotted versus the measured CTY, showing the validity of the estimation of the intrinsic TOF.

Based on this TOF_i–size relationship, it was concluded that the cobalt particle size for maximum CTY is found at 4.5 nm for 0.5 nm bin size. However, as the theoretical optimum particle size depends slightly on the bin size in the histogram analyses, an overall optimum cobalt particle size of 4.7 ± 0.2 nm is obtained (SI – B).

With the intrinsic surface-specific TOF, CTY values for theoretical mono-sized Co catalysts were calculated as a function of the cobalt particle size and are plotted in Fig. 3A. In the same graph, the activities of the Co/CNF catalysts from Bezemer et al. [6] are displayed, as function of their surface-weighted particle size.

In Fig. 3A, it can be observed that the activity of the optimal Co/CNF catalyst (IEN8) is significantly lower than the theoretical maximum activity found for the optimum Co size. To explain the lower activity of this Co/CNF catalyst, the particle size distribution of this catalyst is plotted in Fig. 3B while the optimum size of 4.7 ± 0.2 nm is included (hedged area). Since the maximum of the size distribution coincides nicely with the hedged area, the lower activity of this Co/CNF catalyst should be attributed to the particle size distribution, rather than the difference in surface-weighted size. Most importantly, since the tail in the size distribution contains a relative large cobalt mass fraction (~60% > 6 nm), a lower activity (3.5×10^{-5} mol_{CO} g_{Co}^{-1} s^{-1}) is found when compared to the theoretical maximum CTY of $(4.5 \pm 0.2) \times 10^{-5}$ mol_{CO} g_{Co}^{-1} s^{-1}. This underlines the need for the synthesis of a catalyst with a narrow particle size distribution close to the optimum Co size in order to approach the maximum FT activity. Hereafter, we report on the synthesis a silica-supported cobalt catalyst to approach to the latter situation and to apply the newly developed "design rules".

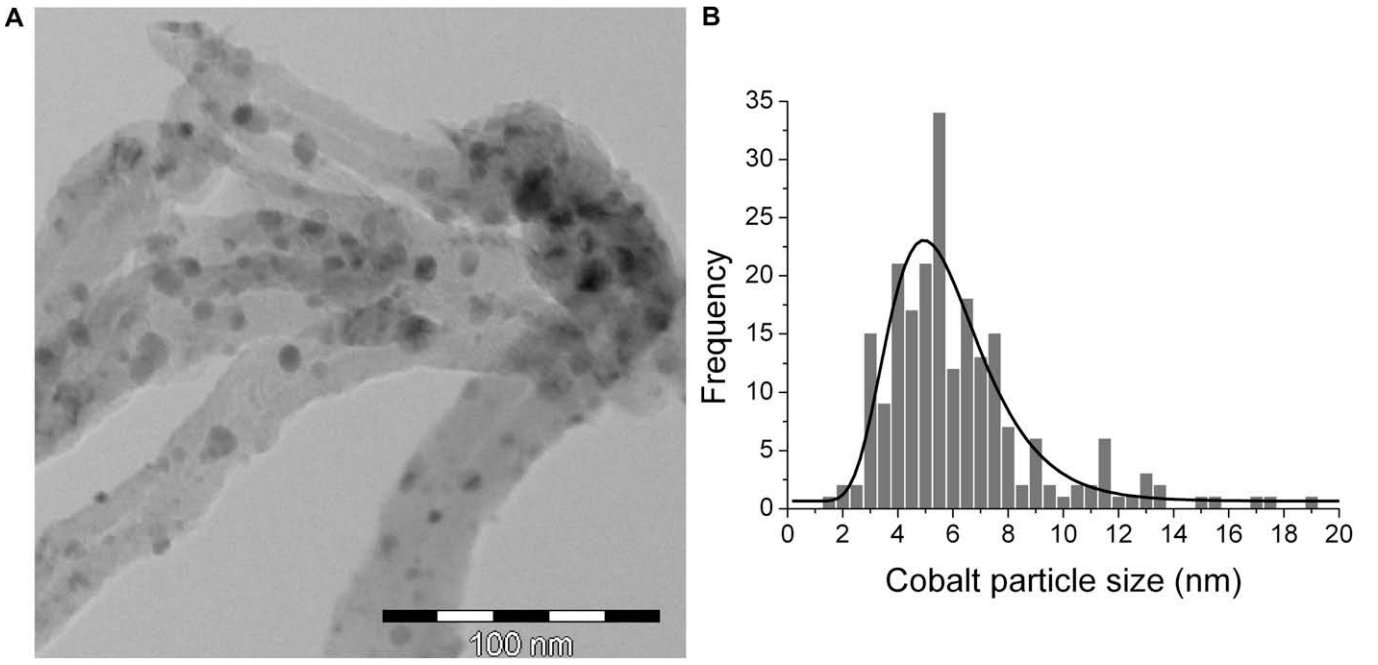

Fig. 1. Example of a TEM image (A) and histogram analysis (B) (0.5 nm bins) for a Co/CNF catalyst (IWN13). The solid line in the histogram graph represents a lognormal fitting curve.

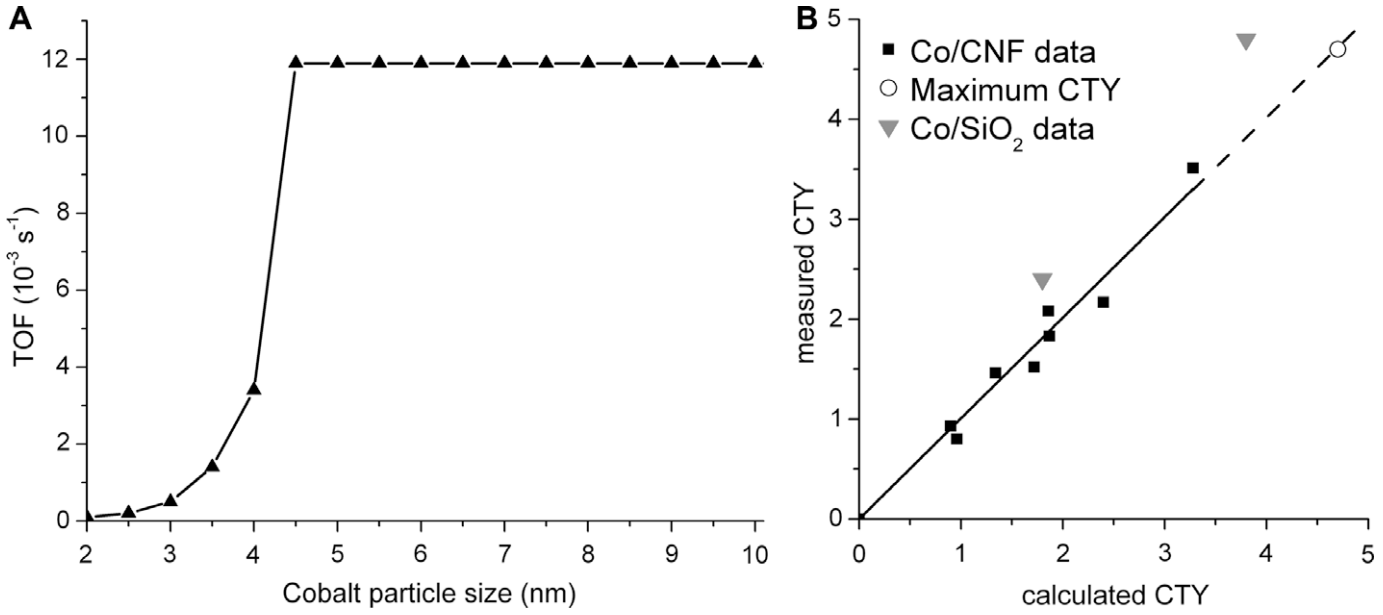

Fig. 2. (A) Estimated intrinsic TOF as function of Co particle. (B) Calculated CTY versus measured CTY of Co/CNF and Co/SiO_2 and theoretical maximum activity (CTY).

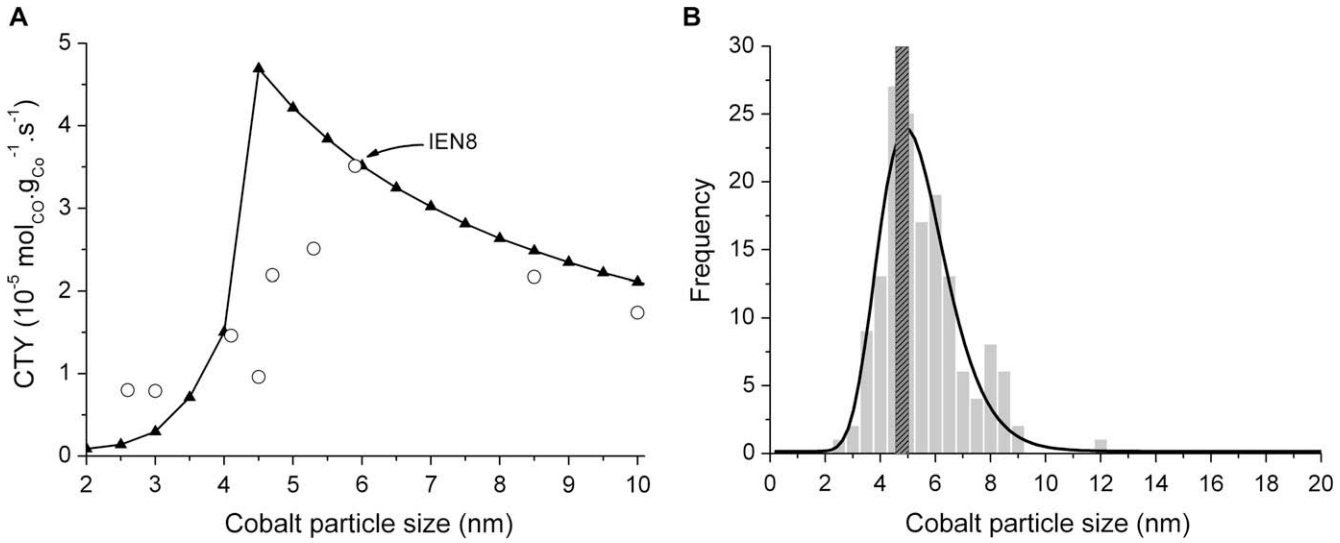

Fig. 3. (A) Calculated CTY based on intrinsic TOF values (triangles). Measured CTY values (○) by Bezemer et al. [2] are added for comparison. (B) Cobalt size distribution of the most active Co/CNF catalyst (IEN8). The hedged area indicates the optimum size of 4.7 ± 0.2 nm.

Table 1
Cobalt on carbon nanofiber catalysts with their preparation details, loadings, particle sizes and FT activities.

Catalyst	Solvent	Precursor	Co loading (wt.%)	XPS[a] (nm)	TEM[b] d_{DW} (nm)	TEM[b] $d_{SW} \pm \sigma$ (nm)	TEM[b] d_{VW} (nm)	FT[c] activity	Selectivity (wt.%)	
									C_1	C_{5+}
IWN13[d]	Water	Cobalt nitrate	13	8.5	6.2	6.9 ± 2.6	7.8	2.17	39	28
IWN12	Water	Cobalt nitrate	12	10	10.8	11.3 ± 3.2	11.8	1.52	38	29
IWN10	Water	Cobalt nitrate	9.9	11	8.3	9.7 ± 5.0	11.6	1.83	43	26
IEN8[d]	Ethanol	Cobalt nitrate	7.5	5.9	5.3	5.7 ± 1.4	6.0	3.51	40	30
IEN4	Ethanol	Cobalt nitrate	3.8	4.6	4.0	4.3 ± 1.3	4.7	2.08	43	27
IWA4[d]	Water	Cobalt acetate	4.2	4.1	2.9	3.2 ± 1.0	3.6	1.46	47	24
IWA1	Water	Cobalt acetate	0.9	2.9	2.7	2.8 ± 0.8	3.0	0.93	56	16
IWA1[d]	Water	Cobalt acetate	1.0	2.6	2.3	2.4 ± 0.7	2.5	0.80	53	18

[a] Based on C and Co XPS signals.
[b] Diameter-weighted (d_{DW}), surface-weighted (d_{SW}) and volume-weighted (d_{VW}) average cobalt particle sizes (nm) after reduction and passivation, including the standard deviation (σ (nm)).
[c] CTY = 10^{-5} mol_{CO} g_{Co}^{-1} s^{-1}.
[d] Catalyst data from Bezemer et al. [6].

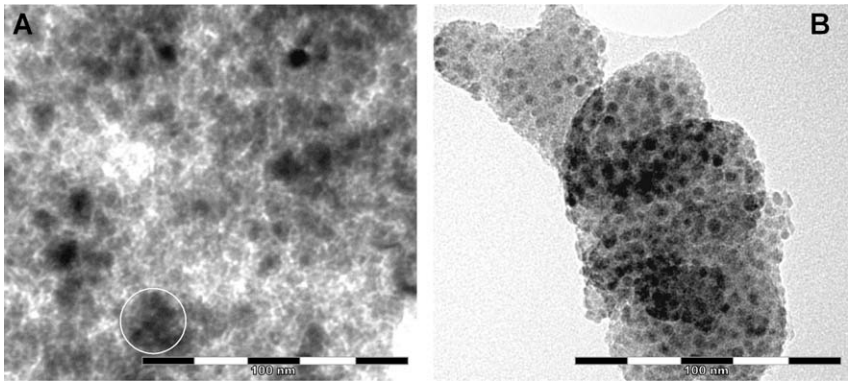

Fig. 4. TEM images of reduced (550 °C) and oxidized AC (A) and NC (B) Co/SiO_2 catalysts.

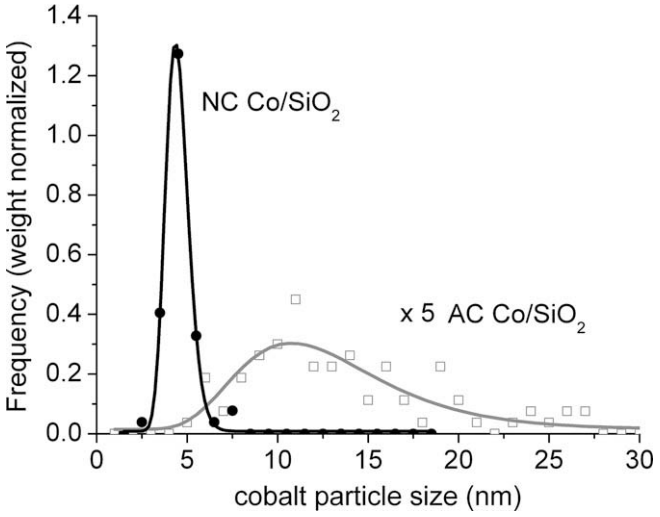

Fig. 5. Cobalt particle size distribution (g_{Co}^{-1}) for reduced (550 °C) and oxidized AC and NC Co/SiO_2 catalysts. The solid lines indicate a lognormal fit to the data.

3.2. Cobalt dispersion of Co/SiO_2 catalysts from TEM analysis

For the preparation of Co/SiO_2 catalysts, a support material with a pore diameter of 6 nm was chosen. This was to ensure that the eventual Co particle size would end up close to the theoretical optimum cobalt size of 4.7 ± 0.2 nm [25,26]. TEM analysis was used to investigate the cobalt particle size and particle size distribution of the air-calcined (AC) and nitric oxide-calcined (NC) Co/SiO_2 catalysts in more detail, after a reduction (550 °C) and oxidation treatment (r.t.).

When comparing the TEM analyses (Fig. 4) of the AC and NC samples, it is clear that NO calcination results in significantly smaller Co particle sizes. Moreover in the case of AC, the Co particles tend to cluster together (cf. inset in Fig. 4A), leaving parts of the silica surface empty. Based on these TEM measurements, a histogram analysis of the cobalt particle size distribution was obtained for the AC and NC samples (Fig. 5).

From this graph, it is evident that a significant narrowing in particle size distribution is obtained with NO calcination (σ = 0.8 nm) when compared to air calcination (σ = 8.1 nm). Moreover, for this NC catalyst, a size distribution was found with a surface-weighted size (d_{SW} = 4.6 nm) close to the theoretical optimum particle size.

Since small Co particles are obtained with NO calcination, reducibility might become an issue [27–29]. Therefore, the degree of reduction of the *in situ* reduced AC and NC catalysts was determined using a principle component analysis of the XANES spectra. These XANES spectra are provided in SI – C.

Table 2
Degree of reduction of AC and NC Co(Pt)/SiO_2 catalysts as obtained from XANES analysis.

Catalyst	Calcination	Reduction temperature (°C)	Degree of reduction after reduction (%)	Degree of reduction after 2 h FT reaction (%)
Co	Air	450	96 ± 5	96 ± 5
Co	NO	450	77 ± 5	88 ± 5
Co	NO	530	82 ± 5	89 ± 5
Co Pt	NO	450	96 ± 5	94 ± 5

From Table 2, it can be seen that the relatively large cobalt oxide crystallites as obtained with air calcination were fully reduced at 450 °C. However, to achieve a similar degree of reduction for the NC samples, with a smaller Co particle size, a higher reduction temperature (530 °C) was needed. From the nearly complete reduction at 450 °C for the Co Pt catalyst, it can be concluded that the addition of Pt facilitates the reduction significantly. Moreover, exposure to FT conditions for 2 h also increases the degree of reduction, most likely due to the highly reducing environment of H_2 and CO. This phenomenon has been observed earlier for example for Co/Al_2O_3 catalysts [30,31].

3.3. FT reaction with Co/SiO_2 catalysts

The Co/SiO_2 catalysts were tested in the Fischer–Tropsch reaction as described earlier. The FT activities (CTY), methane and C_{5+}-selectivities were determined from the hydrocarbon production. An overview of the FT results is provided in Table 3.

For the FT synthesis performed at 1 bar and using NO and air-calcined Co/SiO_2 catalysts, it can be concluded that NO calcination has a tremendous positive impact on the activity, since the CTY increases by a factor 2. This originates from a more narrow size distribution with an average Co size close to the optimum calculated Co particle size. However, a higher methane and lower C_{5+}-selectivity is found for NO-calcined catalysts in line with results of Holmen and co-workers. The latter authors have shown that the aggregation of Co particles lead to higher C_{5+} selectivity [25]. For isolated Co nanoparticles, additional promoter elements might be mandatory for high C_{5+} selectivity [32]. The possibility of enhancing C_{5+}-selectivity of small (2–6 nm) Co particles was for example shown by Morales et al. [33]. Also, current research focuses on the promotion of the NC Co/SiO_2 catalysts.

3.4. Optimum cobalt particle size – theory and practice

In the first part of this paper, the need for a narrow Co particle size distribution with an average size of 4.7 ± 0.2 nm was derived.

Table 3
FT activity and selectivity and particle sizes for Co/CNF, NC and AC Co/SiO_2 catalysts as function of treatment and support material (220 °C, H_2/CO = 2 v/v, 1 bar).

Catalyst	Calcination environment	Reduction time, temperature (°C)	Co_3O_4 crystallite size (nm)[a]	Co particle size (nm)[b]	CTY (10^{-5} mol_{CO} g_{Co}^{-1} s^{-1})	Selectivity (wt.%)	
						C_1	C_{5+}
Co/CNF (IEN8)	Air	2 h, 350	7	5.7 ± 1.4	3.51	40	30
Co/SiO_2	Air	2 h, 550	11	15.8 ± 8.1	2.41	17	57
Co/SiO_2	NO/He	2 h, 550	5	4.6 ± 0.8	4.80	28	35
Co Pt/SiO_2	NO/He	2 h, 450	5	4.7 ± 0.8	4.85	30	32

[a] As determined with XRD ($2\theta = 43°$).
[b] Average cobalt particle size (d_{SW}) from TEM analysis determined after reduction and passivation.

By applying an NO calcination treatment of a Co/SiO_2 catalyst, we met this requirement. The significantly higher activity found for this catalyst when compared to Co/CNF catalysts was ascribed to the more narrow size distribution combined with a surface-average size close to the theoretical optimum. However, if the intrinsic TOF_i values (Fig. 2A) are used together with the size distribution shown in Fig. 5, the expected CTY value equals 3.8×10^{-5} mol_{CO} g_{Co}^{-1} s^{-1}, which is lower than the measured value of 4.8×10^{-5} mol_{CO} g_{Co}^{-1} s^{-1}. The fact that a higher value than the expected value is observed (Fig. 2B) might be due to a promoting effect of an oxidic support material [34], since a similar difference is found for the air-calcined catalyst where values of 1.8×10^{-5} mol_{CO} g_{Co}^{-1} s^{-1} (calculated) and 2.4×10^{-5} mol_{CO} g_{Co}^{-1} s^{-1} (measured) were found (Fig. 2B). This might be an electronic promotion effect like has been observed after the addition of transition metal oxides to cobalt catalysts [32]. However, distribution broadening due to the error in the TEM size measurements (~15%) will affect the activity calculations too. Finally, it might also indicate that the optimum Co particle size is somehow support dependent and is smaller for silica than CNF. This could result from different interactions between the cobalt particles and either the silica or CNF material, which possibly influences the cobalt particle shape as well. A smaller optimum size on silica, though, is in contrast with results found at high FT pressures, which showed a larger optimum Co particle size (10 nm) for Co/ITQ2 catalysts [35] than Co/CNF catalysts, which showed an optimum size of 8 nm [6].

Next to the catalyst properties, the optimal Co particle size is also dependent on the FT process conditions like pressure and temperature. Bezemer et al. [6] already showed that the optimum Co particle size might shift to somewhat higher values for high pressure FT experiments. Therefore, it would be of interest to synthesize catalysts with a larger average Co size, showing similar narrow size distributions. For FT tests at elevated syngas pressures, however, significant partial pressures of water at high conversions have a strong influence on Co/SiO_2 catalysts [36], which might change the optimum Co size. Finally, the addition of promoter elements might influence the maximum activity as well. Aim of the current work, though, was to provide a methodology for the enhancement of the activity of catalysts rather than providing an extensive study toward an optimum size at various test conditions. For the optimal cobalt particle size for the selectivity, although outside the scope of this paper, a similar study is advocated.

4. Conclusions

Cobalt on carbon nanofiber catalysts were successfully applied as a model system to deduce the contribution of Co particles with a specific size to the overall Fischer–Tropsch (FT) activity. From histogram analyses of cobalt particle size distributions and activity measurements, the intrinsic activity for specific cobalt sizes was estimated. Using this analysis, an optimum cobalt particle size of 4.7 ± 0.2 nm and a concurrent maximum activity $(4.5 \pm 0.2) \times 10^{-5}$ mol_{CO} g_{Co}^{-1} s^{-1} was calculated for Co/CNF catalysts in the FT reaction (1 bar and 220 °C). From the comparison of the activities of the theoretical mono-sized and the Co/CNF catalyst found by Bezemer et al., it was concluded that the Co particle size distribution rather than a difference in surface-average particle size causes the lower activity for the Co/CNF catalyst.

Furthermore, a silica-supported catalyst with a narrow Co particle size distribution with a surface-average size of 4.6 ± 0.8 nm was synthesized via NO calcination. This catalyst displays an unprecedented high FT activity and outperforms the air-calcined Co/SiO_2 catalysts at 220 °C, 1 bar. The high activity at 1 bar is ascribed to narrowing of the size distribution close to the optimum. Although a moderate reducibility was found for the small Co particles obtained via the NO calcination, the addition of Pt facilitated the reduction significantly.

Acknowledgments

The authors acknowledge beamline scientists from beamline C, DESY synchrotron with their help on conducting the XAS experiments. S. Menda Ginteng is thanked for her help with preparation of some Co/CNF catalysts. Dr. G.L. Bezemer is acknowledged for TEM and FT data. Shell Global Solutions is thanked for funding of this research.

Appendix A. Supplementary data

TEM images and Co particle size histograms, with an extended description of the applied methodology for the calculation of the optimum Co particle size and XANES spectra of *in situ* reduced Co/SiO_2 catalysts. Supplementary data associated with this article can be found, in the online version, at doi:10.1016/j.jcat.2009.12.015.

References

[1] R.C. Reuel, C.H. Bartholomew, J. Catal. 85 (1984) 78.
[2] L. Fu, C.H. Bartholomew, J. Catal. 92 (1985) 376.
[3] A.S. Lisitsyn, A.V. Golovin, V.L. Kuznetsov, Y.I. Yermakov, C1 Mol. Chem. 1 (1984) 115.
[4] A.S. Lisitsyn, A.V. Golovin, V.L. Kuznetsov, Y.I. Yermakov, J. Catal. 95 (1985) 527.
[5] A. Barbier, A. Tuel, I. Arcon, A. Kodre, G.A. Martin, J. Catal. 200 (2001) 106.
[6] G.L. Bezemer, J.H. Bitter, H.P.C.E. Kuipers, H. Oosterbeek, J.E. Holewijn, X. Xu, F. Kapteijn, A.J. Van Dillen, K.P. de Jong, J. Am. Chem. Soc. 128 (2006) 3956.
[7] J.P. den Breejen, P.B. Radstake, G.L. Bezemer, J.H. Bitter, V. Frøseth, A. Holmen, K.P. de Jong, J. Am. Chem. Soc. 131 (2009) 7197.
[8] A.J. Van Dillen, R.J.A.M. Terörde, D.J. Lensveld, J.W. Geus, K.P. de Jong, J. Catal. 216 (2003) 257.
[9] J. Panpranot, S. Kaewkun, P. Praserthdam, J.G. Goodwin Jr., Catal. Lett. 91 (2003) 95.
[10] T. Mochizuki, T. Hara, N. Koizumi, M. Yamada, Appl. Catal. A – Gen. 317 (2007) 97.
[11] W.T.L. Lim, Z. Zhong, A. Borgna, Chem. Phys. Lett. 471 (2009) 122.
[12] A. Martinez, G. Prieto, J. Catal. 245 (2007) 470.
[13] T. Herranz, X. Deng, A. Cabot, J. Guo, M. Salmeron, J. Phys. Chem. B 113 (2009) 10721.

[14] J.R.A. Sietsma, J.D. Meeldijk, J.P. den Breejen, M. Versluijs-Helder, A.J. van Dillen, P.E. de Jongh, K.P. de Jong, Angew. Chem. Int. Ed. 46 (2007) 4547.
[15] J.R.A. Sietsma, J.D. Meeldijk, M. Versluijs-Helder, A. Broersma, A. Jos Van Dillen, P.E. de Jongh, K.P. de Jong, Chem. Mater. 20 (2008) 2921.
[16] J.R.A. Sietsma, H. Friedrich, A. Broersma, M. Versluijs-Helder, A. Jos van Dillen, P.E. de Jongh, K.P. de Jong, J. Catal. 260 (2008) 227.
[17] M.K. Van der Lee, A.J. Van Dillen, J.W. Geus, K.P. de Jong, J.H. Bitter, Carbon 44 (2006) 629.
[18] O. Kitakami, H. Sato, Y. Shimada, F. Sato, M. Tanaka, Phys. Rev. B 56 (1997) 13849.
[19] J.R. Anderson, Structure of Metallic Catalysts, Academic Press, New York, 1975. p. 359.
[20] C.G. Granqvist, R.A. Buhrman, J. Catal. 42 (1976) 477.
[21] H.P.C.E. Kuipers, Solid State Ionics 16 (1985) 15.
[22] H.P.C.E. Kuipers, H.C.E. Van Leuven, W.M. Visser, Surf. Interface Anal. 8 (1986) 235.
[23] M. Vaarkamp, J.C. Linders, D.C. Koningsberger, Physica B 209 (1995) 159.
[24] D.C. Koningsberger, B.L. Mojet, G.E. van Dorssen, D.E. Ramaker, Top. Catal. 10 (2000) 143.
[25] Ø. Borg, S. Eri, E.A. Blekkan, S. Storsæter, H. Wigum, E. Rytter, A. Holmen, J. Catal. 248 (2007) 89.
[26] A.Y. Khodakov, Catal. Today 144 (2009) 251.
[27] A.Y. Khodakov, J. Lynch, D. Bazin, B. Rebours, N. Zanier, B. Moisson, P. Chaumette, J. Catal. 168 (1997) 16.
[28] G. Jacobs, T.K. Das, Y. Zhang, J. Li, G. Racoillet, B.H. Davis, Appl. Catal. A – Gen. 233 (2002) 263.
[29] J.S. Girardon, E. Quinet, A. Griboval-Constant, P.A. Chernavskii, L. Gengembre, A.Y. Khodakov, J. Catal. 248 (2007) 143.
[30] J. van de Loosdrecht, B. Balzhinimaev, J.A. Dalmon, J.W. Niemantsverdriet, S.V. Tsybulya, A.M. Saib, P.J. van Berge, J.L. Visagie, Catal. Today 123 (2007) 293.
[31] A.M. Saib, A. Borgna, J. van de Loosdrecht, P.J. van Berge, J.W. Niemantsverdriet, Appl. Catal. A – Gen. 312 (2006) 12.
[32] F. Morales, B.M. Weckhuysen, Catalysis (R. Soc. Chem.) 19 (2006) 1.
[33] F. Morales, E. de Smit, F.M.F. de Groot, T. Visser, B.M. Weckhuysen, J. Catal. 246 (2007) 91.
[34] C.H. Bartholomew, R.C. Reuel, Ind. Eng. Chem. Prod. Res. Develop. 24 (1985) 56.
[35] G. Prieto, A. Martínez, P. Concepción, R. Moreno-Tost, J. Catal. 266 (2009) 129.
[36] S. Krishnamoorthy, M. Tu, M.P. Ojeda, D. Pinna, E. Iglesia, J. Catal. 211 (2002) 422.